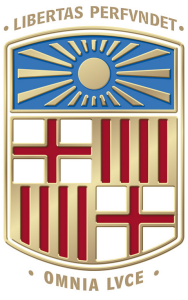

University of Barcelona

Master in Quantum Science and Technology

Cavity-Enhanced Non-destructive Measurement of Magnetic Observables in Cold Atomic Ensembles

Diana Méndez Avalos

Supervisors:

Prof. Morgan Mitchell

Dr. Daniel Benedicto

Institute of Photonic Sciences

Barcelona, 2023

Cavity-Enhanced Non-destructive Measurement of Magnetic Observables in Cold Atomic Ensembles

Diana Méndez Avalos

Supervised by: Prof. Morgan Mitchell and Dr. Daniel Benedicto

ICFO, 08860 Castelldefels (Barcelona), Spain
July 2023

Faraday rotation measurements (FRM) are highly valuable due to their potential to behave as quantum non-destructive measurements under certain conditions. Moreover, applying FRM to Bose-Einstein condensates (BEC) offers significant insights into the magnetic properties, dynamics, and quantum phenomena of the condensate.

To optimize FRM on a BEC, we have implemented an optical cavity that maximizes the interaction between atoms and light. In this work we present a frequency locking system for a 780nm probe laser implementing a Maximum Search Algorithm in a microcontroller Arduino UNO. The implementation of this system has yielded promising results, reducing the noise after the cavity by $\sim$ 20dB compared to the system without the algorithm. Consequently, we can approach the shot noise limit more closely, stabilizing the set-up for the Faraday rotation measurements.

Keywords: Quantum Non-Destructive measurements, Frequency Locking System, Arduino, Ultra cold ensembles.

Diana Méndez Avalos: diana.mendez@icfo.eu

Acknowledgements

I want to thank my supervisors Prof. Morgan Mitchell for his guidance and support and to Dr. Daniel Benedicto for the infinite patience in the lab and for teaching me all the tricks, procedures and insights. Last but not least to Ph.D. candidate Enes Aybar that helped me every day in the lab. Without all of you I would not have lasted at the lab. Thanks to ICFO for allowing me to work in the lab and for the support to all the community.

I also want to thank my parents Alejandra and Rodolfo for their support and advice even at a distance. To my family, thanks for believing in me and for your best wishes always, you always encourage me to keep going.

To all my friends, thank you for being so supportive every day. Specially to Alma, Zarco, Vera and Sara for your "chismecito" and life advice that make me feel never alone wherever I am. I want to give a special thank you to Alberto; you make me feel happy and loved, without you this journey would have been way more difficult to accomplish, I love you.

Finally, I would like to thank Bécalos for believing in me and giving me the economic support to accomplish my master studies.

Contents

1 Introduction

With the advances of quantum sensing and metrology, new techniques in non-destructive measurements have been developed. In particular, low-frequency magnetic fields have been of interest. This has an impact in several areas of knowledge that goes from the understanding of the human mind [BMS+17] to the creation of the universe [AEJ+16]. For instance, with the development on magnetometry techniques we are now capable of detecting magnetic fields at the scale of femto-Teslas [MP20]. All those applications rely on the precise measurement of physical quantities such as the strength of a field, a force, or time [PSO+18].

At the scales at which quantum effects become significant, we need to consider the Heisenberg uncertainty principle. To measure an observable we need to disturb the system that we are interested in. To minimize the disturbance of the measurement to the system, we can rely on a secondary system, that will work as a proxy, that is correlated with the main one in the features that we want to know. In this way we can measure the subsystem without destroying entirely the former. This is an indirect measurement, and is called QND if the system and the measured value of the observable are conserved after the measurement [PSO+18]. Although the idea of QND was starting to develop since the 30's with the early foundations of quantum mechanics, it was not broadly implemented until gravitational wave detection became a research field of interest in the 80's [BK96, GLP98].

As we are interested in the measurements of the magnetization of a medium, there have been some approaches to measure this regime, being Faraday rotation measurements in atomic ensembles one of the most promising approaches [BKR+00]. As these are dispersive measurements, they can behave as QND under the appropriate conditions. Moreover, with the implementation of enhancement techniques, such as optical cavities, we can gain measurement sensitivity. This can result in an improvement of one order of magnitude comparing with previous measurements [BCN+14, MOG+21]. This type of enhancement techniques are then crucial for advancing quantum metrology beyond proof-of-principle experiments [CBW+14]. Furthermore, it was recently found by Mitchell in [MP20] that a Bose-Einstein condensate (BEC) magnetometer can have an energy resolution per bandwidth below $\hbar$ contrary of which what was found for other systems (NVD, SQUID, OPM, etc.) in the past.

In [MOG+21] a novel cavity-enhanced measurement scheme was demonstrated to boost the sensitivity of polarization rotation measurements produced by an atomic medium. This type of measurements are also known as Faraday rotation measurements. A quasi-concentric optical cavity was implemented to increase the atom-light coupling. It was demonstrated that their detection is photon shot noise limited. However, as compared to schemes without the cavity, they show that the cavity contributes to also boost the technical noise of the detection, limiting the shot noise limited region of the probing scheme. There are several reason to explain this behaviour. The first one is that the implementation of the cavity introduces more technical noise with the addition of several optical elements. The second one is that it was observed that the environmental conditions of the laboratory strongly influence the relative optical path length in the set-up.

In figure 1 extracted from [Maz23], it is shown the changes in the percentage of relative humidity and the variations of the frequency of an Acousto Optical Modulator (f_{AOM}) during the time of the day in hours. The relative humidity was measured with an hygrometer placed next to the piezoelectric that modulates the optical cavity length. The f_{AOM} refers to the changes in the frequency where the probe laser was resonant with the cavity. Those changes were measured by scanning on frequency the cavity to find the probe laser's

resonant frequency. As the AOM's frequency is controlled by a voltage controlled oscillator (VCO), the voltage can be fixed at the frequency in which the laser is resonant according to the scan. Further details in the measuring scheme can be found in [Maz23].

In this figure we can observe a direct correlation between the relative humidity and the frequency variation. This means that along the day there will be a change in the cavity length due to environmental conditions, and thus changing the optical path length of the probe laser. Thus, the laser requires a restabilization of frequency. As we will see in section 3.2, the optical cavity is designed to be on transmission, which make unfeasible the implementation of standard locking techniques on the probe laser.

In this work, we address the effect of the laboratory conditions on the detection scheme, i.e., we implement a stabilization system that can track the relative changes between the frequency of the probe light and the resonant frequency of the cavity.

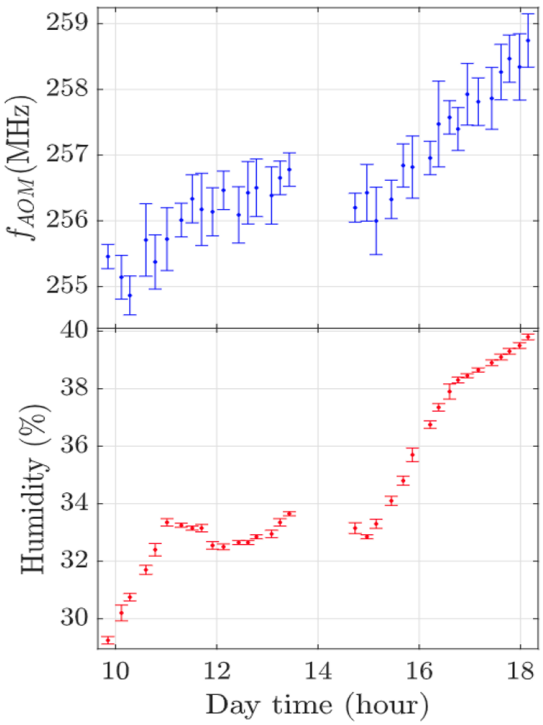

Figure 1: Laboratory's percentage relative humidity (in red) and Acousto Optical Modulator's frequency (f_{AOM}) (in blue) variation during the time of day. Relative humidity data show mean and standard deviation over 4 measurements. AOM frequency data points are mean and standard deviation obtained from the frequency scan fit. Plot obtained from [Maz23]

.

1.1 Objectives

1.1.1 General Objectives

- To stabilize probe frequency with respect to the cavity length using the transmitted intensity.
- To measure magnetic observables in a cold atomic ensemble using an optical cavity

1.1.2 Specific Objectives

- Design of a Maximum Search Algorithm using a micro-controller Arduino

- Evaluate the performance of the algorithm in a test set-up for a given frequency noise spectrum.
- Implement the algorithm to stabilize the frequency of the probe laser in the main experiment
- Observe a reduction of the technical noise in cavity-enhanced Faraday measurements

2 Theoretical background

Before getting to the description of the work, we are going to introduce the theoretical background to have a better understanding of the sensitivity of an atomic magnetometer and how the detection noise enters the description.

To study the magnetic properties of a cold atomic ensemble, we will use an induced birefringence on the resonance levels of the atoms. This will interact as the classical Faraday effect: when linearly polarized light propagates through a medium parallel to an externally applied magnetic field, the plane of polarization undergoes a rotation, mimicking the optical activity observed in certain materials [Gue90]. On the other side, in the quantum limit, we will refer to the Faraday rotation measurement as a dispersive measurement in which far-off resonant probe light is sent with a given polarization through the atomic medium. This probe light interacts with the atoms, changing its polarization. This change is measured to acquire knowledge of the atomic system without disturbing it too much [BK96]. In this way, we can detect optically precise measurements of an external magnetic field detecting the Larmor precession produced in the cold atomic ensemble [BK13]. This can be done as the cold ensemble is a spin-polarized atomic sample after the induced birefringence.

In quantum mechanics, the description of the state of polarization of a plane wave can be made using the Stokes operators:

$$\hat{\mathcal{S}}_\mu = \frac{1}{2}(\hat{a}_+^*\hat{a}_-^*)\sigma_\mu(\hat{a}_+\hat{a}_-)^T \tag{1}$$

where $\hat{a}_\pm$ are the annihilation operators, $\hat{a}_\pm^*$ its complex conjugate and σ_μ are the Pauli matrices for $\mu = x, y, z$ and the identity for $\mu = 0$.

With the Stokes operators we can understand the expected value of each one ($\mu = x, y, z$) as half the difference in the number of photons in the different bases (horizontal-vertical, 45° and in the circular basis, respectively), including $\hat{\mathcal{S}}_0$ as one half the total number of photons [Ál17].

We can expand the light-atom interaction Hamiltonian into three main parts of the polarizability tensor: scalar ($H^{(0)}$), vector($H^{(1)}$), and tensor($H^{(2)}$). We are interested in the vectorial part of the Hamiltonian ($H^{(1)}$) as it will contain the main contribution to the birefringence effect. To describe the total interaction between the laser and the entire atomic sample, we need to sum the interaction Hamiltonian for each atom

$$\mathcal{H}_{\text{int}} = \sum^{N} H^{(1)} \tag{2}$$

If we want to express equation 2 in terms of the collective spin operator, we also need take on account that for a many body system it can be defined as the sum of the single atoms orientation operators, i.e.,

$$\hat{F}_i = \sum_j^N \hat{f}_j \tag{3}$$

with $i = x, y, z$ and N the number of atoms. Then, this will allow us to redefine the interaction Hamiltonian as

$$\mathcal{H}_{\text{int}} = \frac{\hbar G_1}{\tau_p}\hat{\mathcal{S}}_z\hat{F}_z \tag{4}$$

with τ_p the total interaction time and G_1 the dimensionless coupling factor. This variable accounts for both the polarizability and the geometrical factors that modify the effective interaction strength between the light and the ensemble.

Quantum noise, which exists in both the optical measurement and the atomic system, imposes an inherent limitation on the detection of the Larmor precession. Taking into account the Heisenberg uncertainty relationships, we can only achieve the knowledge of one observable without losing all information of the other one. For the case of Faraday rotation, we can write the spin resolution in terms of the uncertainty in the number of photons and the coupling factor [Ál17]:

$$\Delta\hat{F} = \frac{\Delta\theta}{G_1} = \frac{1}{\sqrt{\hat{\mathcal{S}}_0}G_1} \tag{5}$$

where $\hat{F}$ is the number of spins, θ the rotation angle, G_1 the coupling factor and $\hat{\mathcal{S}}_0$ the number of photons

With this relationship we can then estimate the rotation angle from the atoms with the number of photons that interact with the condensate. This type of measurements are called quantum non-destructive measurements (QND) under some conditions. They allow magnetometry to surpass the standard quantum limit $\delta B \propto 1/\sqrt{N}$, with N the number of atoms, from the atomic projection noise [KNDM10].

One important feature in the development of QND technologies is the stabilization of the system so we can reach precision measurements. The most studied and developed QND technologies are done in optical systems. Here the required stabilization is for paths and cavity lengths.

There has been several approaches develop through the years for this purpose. For example, The Pound-Drever-Hall (PDH) technique is commonly used nowadays in optical labs. It is an optical frequency discriminator and laser stabilization system based on signals reflected from a stable Fabry-Perot reference interferometer [DHK+83]. It involves splitting the laser beam into a signal and a local oscillator beam, modulating them with a reference signal, combining them, and directing them back into the laser cavity to create an optical feedback loop. The interference between the beams is detected, demodulated, and used to generate an error signal, which is then used to adjust the laser's frequency. This technique allows precise locking of the laser to a specific reference frequency [Bla01].

In recent years other types of digital locking systems has been implemented for optics experiments. With the development of digital technologies as Field Programable Gate Array (FPGA) and Microcontroller units (MCU), the number of applications have been rise due to the low cost of these devices [HJR+14, SCP+11, DB09].

3 Results

The results section is divided into two main parts. In the first one we will describe the development and test set-up for the Maximum Search Algorithm and its efficiency. In the second one the description of the main experimental set-up is presented in conjunction with the characterization of the optical cavity and the implementation set-up for the algorithm. Finally, the discussion of the performance of the algorithm is discussed.

3.1 Locking system

In order to implement the locking system, a maximum search algorithm was implemented to search the resonance frequency with the cavity. Additionally, two setups were implemented: one for testing and one within the main experiment.

3.1.1 Maximum Search Algorithm

The objective of the Maximum Search Algorithm is to search for the frequency at which the probe laser is on resonance with the cavity. This will be reflected in the intensity measured by a photo-detector (PD) placed after the cavity. If the laser is on resonance, the intensity will be maximum. When the laser passes through the AOM, the resulting beam has the frequency of the sum of the laser plus the frequency of the 1st mode of the laser. Thus the MSA changes the frequency of the AOM such that the reading from the PD is maximum.

Before implementing the algorithm, we first set the AOM at its resonance frequency ν_0. Then, the transmittance after the cavity is measured at different frequencies of the laser. After that, we find the frequency ν_l at which the transmitted intensity is the highest (Y_{max}), i.e., the laser is on resonance with the cavity, and fix the frequency at ν_l.

After setting ν_0, the algorithm can start working. The maximum search algorithm (MSA) is then illustrated in figure 2. On each cycle it will take the mean value of the power over 25 readings of the PD at ν_0. We will call this value Y_1. If $|Y_{max} - Y_1| > \epsilon$, where ϵ is a threshold value, the algorithm will trigger to start searching again for the maximum power. If not, the MSA will not correct the frequency ν_0.

When the algorithm is triggered, then it compares the intensity value Y_1 with the PD reading Y_2 at $\nu_0 \to \nu_0 + \Delta\nu$. Depending if the new value Y_2 is greater or lower, the algorithm will add or subtract $\Delta\nu$ to ν_0 respectively until it reaches the maximum intensity. Then the algorithm will lock the new AOM's frequency ν_0 where we have now a new Y_{max}. This will repeat each time $|Y_{max} - Y_1| > \epsilon$.

The MSA has the limitation of the electronic noise coming from the PD. The noise can make MSA to find a local maximum instead of the global one that we are searching for. Because of this, we optimized the parameters $\Delta\nu$ and ϵ to see beyond the noise. However, we still introduced a new variable γ that will be a noise threshold when comparing two consecutive PD readings.

Moreover, if there is a sudden lab change or the algorithm has not been implemented in a long time, the maximum intensity can be shifted far enough for the noise contribution to become dominant. In this situation, the MSA will start a frequency scan of the AOM until it finds the peak again. The MSA will then set ν_0 at the lowest bound of the AOM's frequency range. From there it will increment $\Delta\nu$ and compare Y_2 and Y_1 until it reaches ν_0 such that $|Y_2 - Y_1| > \gamma$. Finally, the algorithm can return to the main search in the loop.

The algorithm was implemented in the microcontroller Arduino's integrated development environment (see Appendix A).

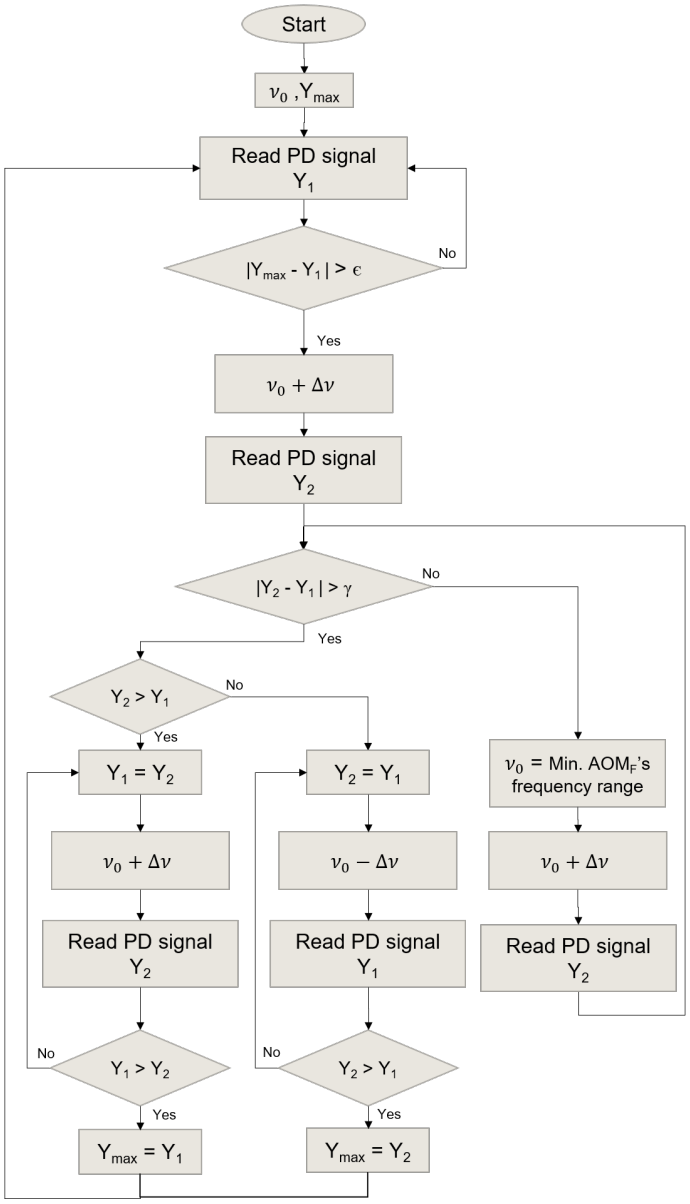

Figure 2: Flow diagram of the Maximum Search Algorithm

3.1.2 Testing setup

In this section we describe the set-up and the efficiency test results that we get from the MSA.

The test setup as shown in figure 3 consists of an Acousto Optic Modulator (AOM) (Crystal Technology: 3110-125), labeled AOM_F in the figure, in a double pass configuration.

We implemented first a single-pass AOM configuration. It was observed that when scanning the AOM frequency the range of beam deflections was large and caused the beam to miss the detector. To avoid such beam deflections, a double-pass AOM was then implemented, and used for the remainder of the experiments. The AOM_F is driven with an

RF signal coming from a voltage-controlled oscillator (Mini-Circuits: VCO ZOS-150+), a voltage-variable attenuator (Mini-Circuits: VVA ZX73-2500-S+), a switch (Mini-Circuits: ZAWA-2-50DR+) and an amplifier (Mini-Circuits: ZHL-1-2W-S+)

The tuning voltage to change the frequency of the VCO is generated using an Arduino UNO and a shield with ADC and DAC inputs and outputs (Diligent, Analog Shield). The DAC module can generate a DC signal of ±5V. The VVA was fed with an external supply of 15V. The electric signal produced by the VCO has an power of -0.73dBm at 120MHz (the resonant frequency of the AOM) after the VVA, before being injected into the amplifier.

To test the MSA in this setup we first change manually the VCO's external supply to see if the algorithm corrected the change. We observed that the MSA managed to find the global maximum. It was able to find it in a range between 20 and 100 ms depending on how much and how fast we manually changed the voltage of the external supply. Although we saw the algorithm worked in this situation, an additional source was implemented. We added a noise signal generated with a RedPitaya (STEMlab 125-10) that simulates the cavity changes.

We first added a white noise to the signal, to see the corrections under the noise presence at all frequencies. However, it can be observed in figure 1 that the changes in the optical path laser due to the laboratory conditions happen at low frequencies. This is the frequency range in which we are interested to have a better noise correction. Thus, we implemented in the RedPitaya a Pink noise signal as it has a power spectral density of the inverse of the frequency noise, so the lower the frequency the power will be higher. The pink noise was implemented using the python library "pyplnoise" which is based on the work of Plaszczynski [Pla07].

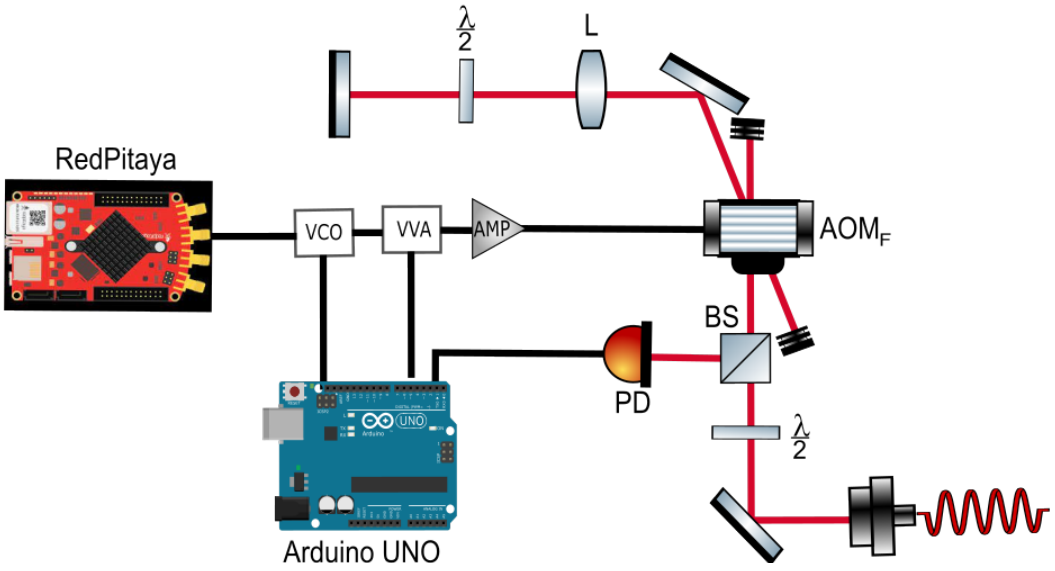

Figure 3: Test Setup. In red, the optical path. In black the electrical wires. The light path is the following. First the light is injected through a fiber laser. The beam will be reflected from a mirror and pass through a $\lambda/2$ wave plate. Then, the beam pass through a beam splitter (BS). The beam splitter will then divide the beam into two equal beams. The one that gets transmitted is injected into an acousto optic modulator (AOM_F). The 0th mode will be blocked meanwhile the 1st mode gets reflected and passes trough a lens (L) and a $\lambda/2$ wave plate. It will be then reflected back into the same path until it reaches the beam splitter (BS). At that point th beam will be reflected from the beamsplitter and will hit the photodetector (PD). The PD signal will be read by the Arduino UNO, which will modify the input voltage of the VCO and the VVA. The VCO also has another input voltage that comes from the RedPitaya. The output RF signal that comes from the VCO and the VVA will be amplified to be injected into the AOM_F.

To evaluate the efficiency of the system, the signal from the photo detector (PD) was connected to a spectrum analyzer. We established the baseline as the electronic noise coming from the PD blocked from the light. Then we let the light hit the PD with the addition of white noise and pink noise. Finally, we measured the signal with the pink noise and the algorithm. The MSA in this case will work in a continuous way, this means that will work constantly at the same time the measurements are taken.

It is worth mentioning that the periodic peaks shown in figure 4 are due to the RedPitaya response. As the RedPitaya analog outputs work by receiving a digital bus of data, the frequency at which you determine the output will be reflected at the Spectrum analyzer. As we can see from figure 4, the signal after the the MSA reduced its baseline signal. To compare the power spectra signals, we calculated the mean of each power spectra from the white and pink noise and compared it with the power spectrum from the signal with the MSA implementation. The noise reduction from the white noise is 17.85dBm, while the noise reduction from the pink noise is 25.37dBm. Then, the implementation of the algorithm is able to reduce the noise. With this result we could then implement the system with the cavity.

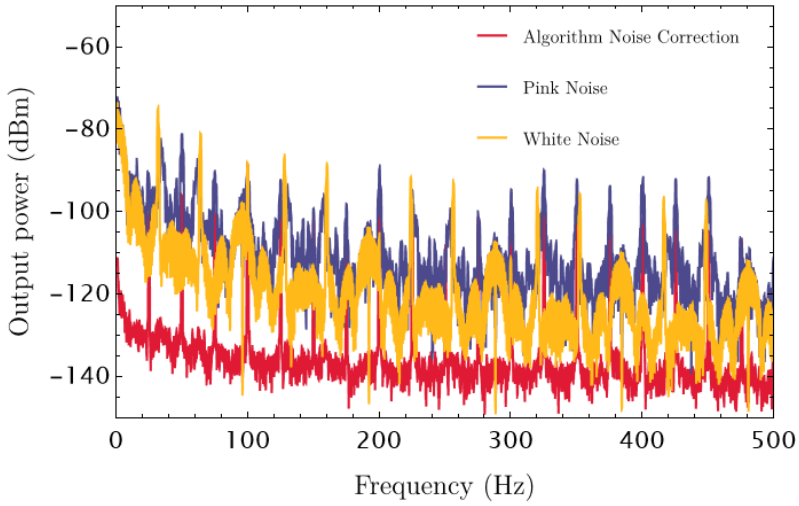

Figure 4: Noise spectrum of the PD signal in a range of 500Hz. In yellow the power spectrum of the PD signal after the addition of white noise to the VCO through the RedPitaya. In purple, the power spectrum of the signal after the addition of the pink noise to the VCO. And in red, the power spectrum of the PD signal after the MSA implementation. The noise reduction of the pink (white) noise power spectrum with the MSA is 25.37dBm (17.85dBm)

3.2 Experimental set-up

As the MSA was implemented in the main experiment, in this section we are going to describe the experimental design before the implementation of the algorithm. Moreover, we are going to describe the characterization of the optical cavity's parameters such as the finesse, length, free spectral range, among others.

The set-up for the cavity-enhanced Faraday rotation measurements with Bose-Einstein condensates is as described in detail by Mazzinghi [Maz23] as shown in figure 5. It consist of two spherical mirrors of radius $r_{oc} = 0.35m$. The mirrors are placed at an equal distance of 0.35m from the center of the vacuum chamber. That will create a quasi-concentric optical cavity. In this configuration the beam waist will be small as it is required to have better atom-light coupling with the condensate placed in the middle of the cavity.

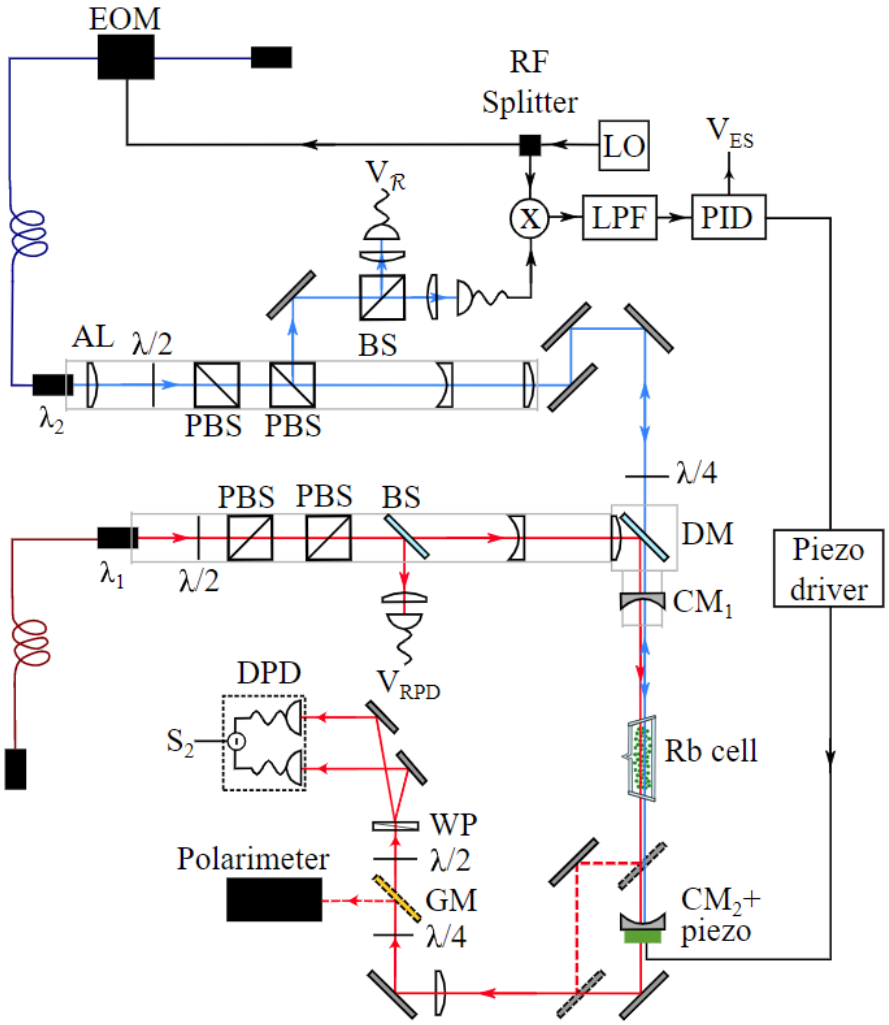

Figure 5: Set-up for the cavity-enhanced Faraday rotation measurements experiment before the implementation of the algorithm. In solid red, the optical path for the 780nm (probe) laser and in blue the optical path for the 1560nm (master) laser. The figure is obtained from [MOG+21], which compared a single pass system to a cavity enhanced one. The counterpart in dashed-red is the single pass laser path, however it will not be used in this work.

Through the cavity two lasers of different wavelength propagate. The first one is a 1560nm master laser and the second one is a 780nm probe laser. The laser light generation is described in PhD thesis of Silvana Palacios [Ál17]. The master laser was chosen for the 780nm laser would be frequency doubled from the 1560nm laser. The 1560nm laser is frequency stabilized by means of spectroscopic techniques. In this way, the laser is low noise and narrow linewidth. The frequency doubling is done with a periodically poled Lithium Niobate (PPLN) non-linear crystal. One part of the generated light is used to lock the laser to the D_2 line by modulation-transfer spectroscopy [dE+15]. The other part of the light is used as a reference to the offset locking of other lasers in the laboratory. The part of the 1560nm light that was not converted, is injected into an AOM to adjust its power and then passed to the experiment.

The cavity is designed to be on reflection for the 1560nm laser light. This light is then use as a reference for the PDH locking technique [DHK+83] to fix the length of the cavity. The PDH will then give feedback to a driver to fix the cavity length by means of a

piezoelectric ring (Piezomechanik: $\text{HPS}_{t150/20-15/12}$), which is attached to one side mirror (CM_2) of the cavity. In this way the 1560nm laser is at resonance inside the cavity. For this configurations the cavity will have R1 = 0.80, R2 = 1.

The second laser light inside the cavity is a 780nm probe laser. To study the magnetic properties of atomic ensembles, the cavity for this laser is on transmission. For this laser the mirrors' reflectivity will be R1 = 0.99, R2 = 0.86. This creates a low finesse cavity. The theoretical values expected for the finesse are 39 ± 4 for the master laser, and 28 ± 3 for the probe one.

Mazzinghi showed in her work that this configuration of the cavity would be the best for the enhancement of the measurements. However, the laser's power is too low to work for a PDH locking. Thus, the error signal is unstable for a PDH locking for the probe laser.

In order to characterize the optical cavity, we first scan the voltage of the cavity using a function generator connected to the piezo driver. The scan was made with a triangular wave voltage at 10Hz and the amplitude was adjusted with the gain of the piezo driver. Then, we search for the maximum power of the TEM_{00} mode of the laser adjusting the mirrors of the cavity. The alignment process for the two wavelengths is as follows: first, we align the cavity with respect to the 780nm (or probe) wavelength to maximize the amplitude of the TEM_{00} mode. Then, we superimpose the 1560nm laser beam on it, trying to maximize also at the power of the TEM_{00} mode.

As shown in figure 6, we recorded the transmitted (reflected) intensity for the probe (master) wavelengths, as well as the error signal generated using a PDH scheme from the reflected signal of the master wavelength. For both lasers, we fit a Lorentzian defined as

$$f_{\mathcal{L}} = \frac{A}{1 + (x - x_0)^2/(\gamma/2)^2} + b \tag{6}$$

where A is the amplitude, x_0 is the center, γ is the full width half maximum, and b is the offset of the peak.

The formula to calculate the Finesse is

$$\mathcal{F} = \frac{\delta\nu_{FSR}}{\Delta\nu_{FWHM}} \tag{7}$$

where $\delta\nu_{FSR}$ is the free spectral range (FSR), and $\Delta\nu_{FWHM}$ is the full width at half-maximum (FWHM) of the transmission resonance, both in frequency units [SD14]. In our case, $\delta\nu_{FSR}$ can be extracted from the fit as the distance between the two peaks, i.e., $|x_0^{(1)} - x_0^{(2)}|$ where $x_0^{(i)}$ is the i-th line center; and $\Delta\nu_{FWHM}$ will be the mean full width half maximum $\bar{\gamma}$. The redefinition from equation 7 for our fit is

$$\mathcal{F} = \frac{|x_0^{(1)} - x_0^{(2)}|}{\bar{\gamma}} \tag{8}$$

For the peaks shown in figure 6 we found a finesse of 17.93 for the probe laser and 11.80 for the master laser. As we see in the figure, we also have some modes besides the TEM_{00} one. This means that spatially our input beam has nonzero overlap with multiple modes, so the mode-matching to the cavity is not perfect. If the cavity would be exactly concentric, the modes would be degenerate. Since the cavity is cuasi-concentric, the modes are not exactly degenerate. However, as long as the TEM_{00} mode has the highest intensity and the finesse is the largest, we will not have problems regarding other modes.

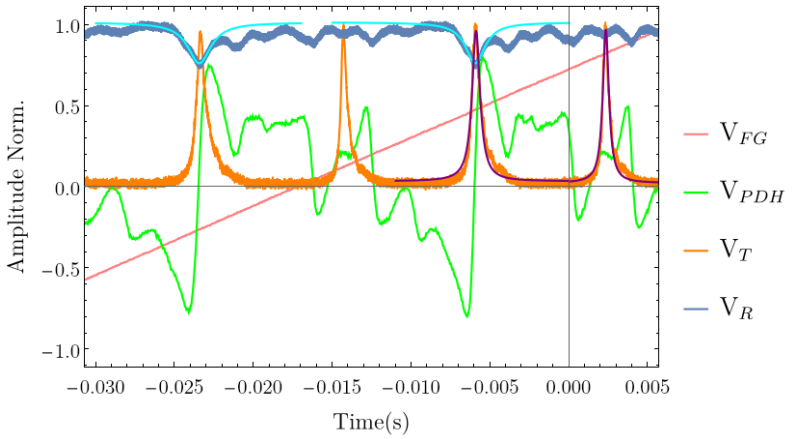

Figure 6: Voltage amplitude normalized during a scan of the cavity length. In orange the transmitted light (V_T) and in blue reflected (V_R) one, the error signal for the PDH in green (V_{PDH}), and the function generator output voltage in pink (V_{FG}). In purple and in cyan are the Lorentzian fits used to calculate the finesse for the probe and master lasers respectively.

As we want the cavity to be concentric for both wavelengths, the cavity needs to be close to $L = 0.7$m that is two times the radious of curvature for the needed mirrors. For this length, the Free Spectral Range (FSR) for an empty standing-wave resonator of length L can be calculated as

$$\Delta\nu_{FSR} = c/2L \tag{9}$$

with c the light velocity constant and $\Delta\nu_{FSR}$ the frequency change. Then if we want L be close to 0.7m our FSR will be around 215 MHz.

To know the precise cavity length, we did a frequency scan of the cavity from a range of 400MHz, as shown in figure 7. With this scan, we get a $\Delta\nu_{FSR} = 215.9 \pm 1.8$ and then we can calculate a length for the cavity using equation 9. The result for this scan is $L = 0.694 \pm 0.006$ m.

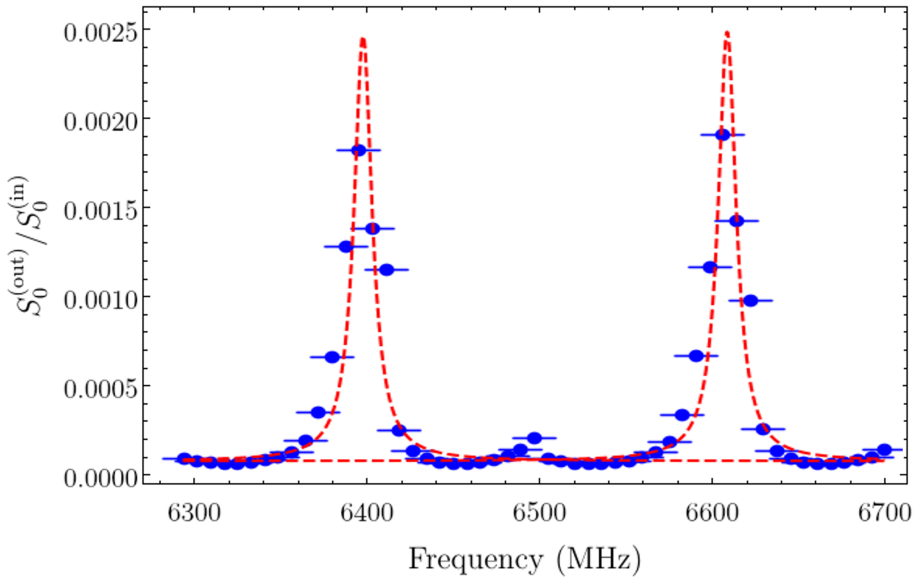

Figure 7: Frequency versus number of photons for the optical cavity scan. In blue the experimental data, and in red the fit data. The parameters for Lorentzian fit for the first peak are $A = 2.405 * 10^{-3}$, $x_0 = 6394$MHz, $\gamma = 13$MHz and $b = 7 * 10^{-5}$; and for the second peak are $A = 2.427 * 10^{-3}$, $x_0 = 6610$MHz, $\gamma = 12.99$ and $b = 7 * 10^{-}5$

Another characteristic of our cavity is the waist beam it can generate. For our case the most important point will be the center of the cavity where is the region in which the light will interact with the atoms. Based on the length obtained by the FSR, we can calculate the corresponding beam waist at the center of the cavity with

$$\mathrm{w}_0^2 = \frac{\lambda L}{2\pi}\sqrt{2\frac{r_{oc}}{L} - 1} \tag{10}$$

where λ is the laser wavelength, L is the cavity length, r_{oc} is the radious of curvature of the mirrors and w_0 is the waist width, that for the parameters we have measured gives a result of $\mathrm{w}_0 = 21.51\mu$m.

3.2.1 Implementation setup

After testing the MSA in a separate set-up, we can now implement the algorithm in the main experimental set-up described in section 3.2. In this section we are going to give the description of the changes made to the main set-up. We also show the results on the measurements made for the MSA performance.

The second setup was implemented within the main experimental set-up previously assembled as in [Maz23] with modifications for the frequency-locking system as in figure 8. The probe laser light is injected into an AOM_F in a double pass setup. The AOM_F subscript means that that laser will be later use for the Faraday rotation measurements. After that, the light is injected in an optical cavity and measured in a photo detector ($\mathrm{PD}_{\mathrm{Lock}}$) after the cavity. Whereas in the first setup we tested the MSA ability to remove "artificial" noise introduced by the RedPitaya, in this setup the noise occurs naturally as we have now the cavity that will generate the noise of our system. Furthermore, the master laser part of the system is the same as in figure 5, but it is not represented in figure 8.

In the previous system, the MSA worked in a continuous way while taking the measurements. In the final implementation set-up we change this configuration as the light to

lock the probe laser is the same light that will work to measure the Faraday rotation. As the power after the cavity is already too low, we do not want to lose any information that comes from the atoms. Besides, the MSA also needs enough power, so the PD readings can be outside the electrical noise.

We then implemented a rotating mirror with a servomotor. The Arduino sends a signal to the servomotor to indicate its rotation. Thus, we now have a final routine as follows. First the software Cicero that controls the main experiment sequence sends a trigger signal to the Arduino. Then Arduino tells the rotating mirror to position down. After that the MSA starts running. Finally when the trigger finishes the mirror position up again.

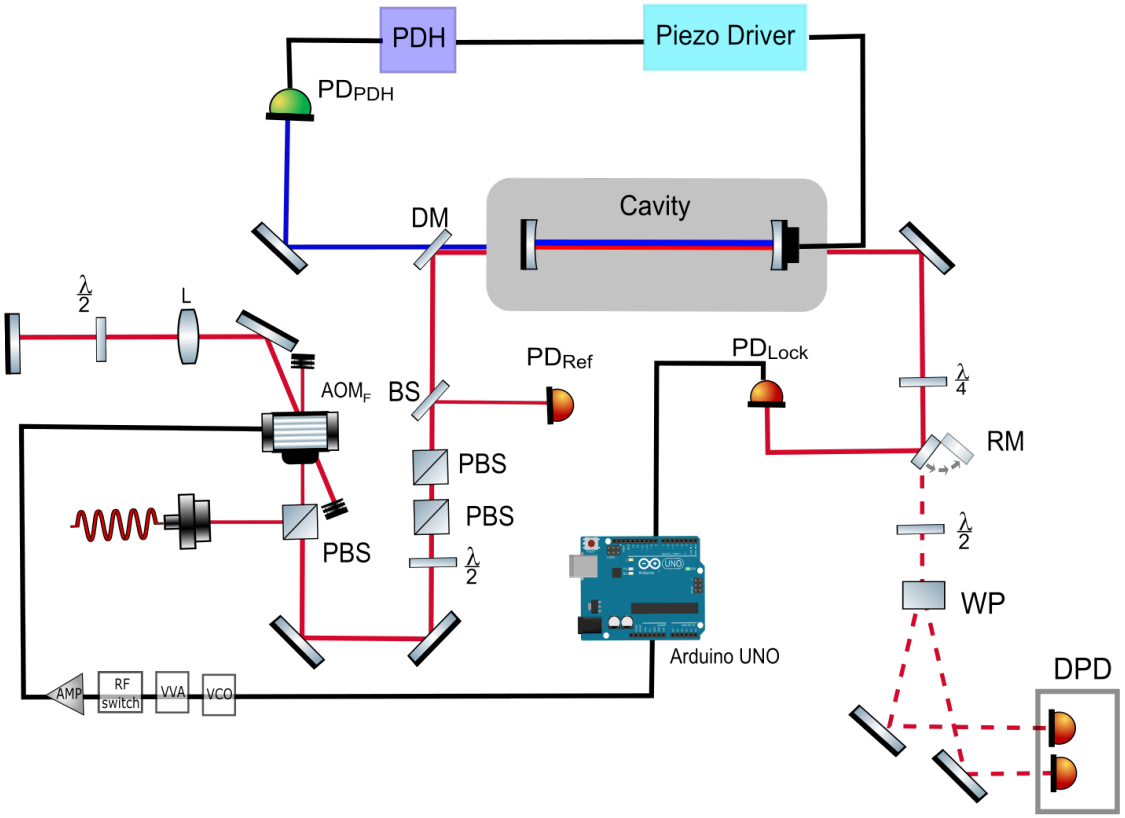

Figure 8: Experimental Setup. In red and in blue, the optical path of the 780nm and 1560nm lasers, respectively. In black the electrical wires. The rotating mirror (RM) connection to the Arduino is not showed in the picture. The path light is the following. First, the light is inserted into the system through an optical fiber. The light is then injected into an AOM_F in a double pass configuration. After that, the light gets reflected into a $\lambda/2$ wave plate and gets through two polarized beam splitters (PBS). The light is then separated by a beam splitter. Half of the light goes to a photodetector (PD_{ref}). The other half is mixed with the 1560nm laser wtih a dichroic mirror (DM). Both of them get injected into the cavity. The 1560nm laser light will be on reflection, while the 780nm one will be on transmission. The 780nm light that gets transmitted is then reflected into a $\lambda/4$ wave plate. The light then can go into two different paths. The first one illustrated as dashed red, gets into a $\lambda/2$ wave plate and gets through a Wollaston prism that will separate the light in a basis of two different polarization, it will be then measured by the differential photodetector (DPD). The second path the transmitted light can follow gets reflected with a rotating mirror and gets measured by a photodetector (PD_{Lock}). Finally, the signal will be used for the MSA by the Arduino which will send the voltage response to the VCO. The signal after the VCO, VVA, a switch and an amplifier will be then injected into the AOM_F that will controll the frequency

In this system we also connected the photo detector output to the Spectrum analyzer and evaluated the power spectrum of the signal with and without the MSA feedback. In order to compare the noise reduction in both set-ups, the algorithm during these measurements works also in a continuous way. As we can see on figure 9, we can see again an overall reduction of the noise baseline. The mean reduction along the frequency range is 15.23dBm after implementing the MSA with the cavity. However, this just gives little information of the performance along the day.

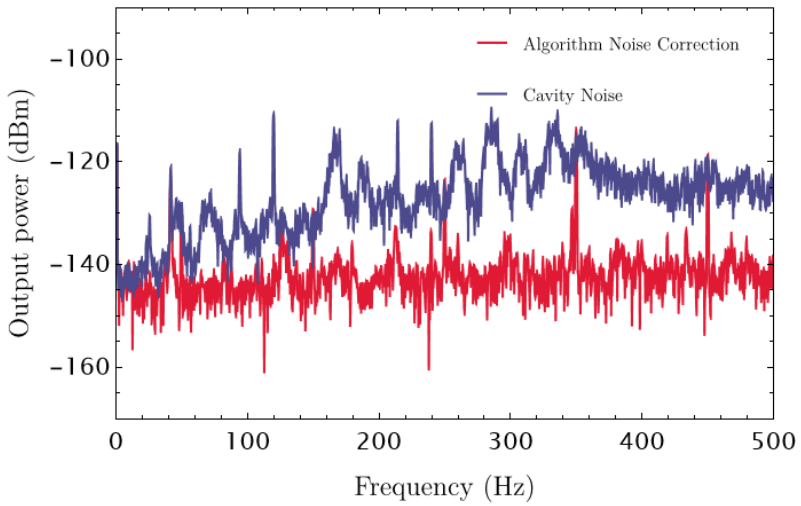

Figure 9: Power spectrum of the noise signal after the cavity before (blue), and after (red) the MSA implementation in a range of 500Hz. The mean noise reduction with the MSA is 15.23dBm

To evaluate the effectiveness of the frequency locking system, the system was run through some hours of the day. We choose to run the sequence each 1.5 minutes for about 2.5 hours. After each cycle the intensity after the cavity and the voltage of the VCO were recorded.

The signal collected after each run was taken with a differential photodetector (DPD) placed after the cavity. This measurement was compared with the reference signal received from the photodetector (PD_{Ref}) before the cavity to have the ratio between the number of photons that go into the cavity and the ones that got out. The DPD is described in [CCSM16]. Basically it is composed of two high quantum efficiency photo diodes connected in series. In this configuration these detectors extract the photo current's difference. If the duration of a light pulse is significantly shorter than the relaxation time, the output signal from the detector exhibits a consistent slope. This slope is directly proportional to the difference in photon numbers detected by the two photodetectors. The DPD is used to measure Faraday rotation. However, in our case we used only one side of the DPD as we are measuring only the cavity transmission. Then the DPD will behave as a photodiode with the property that the calibration of the DPD was well defined for the number of photons by [Maz23]. Furthermore, we want congruent measurements between the transmission and the Faraday rotation measurements.

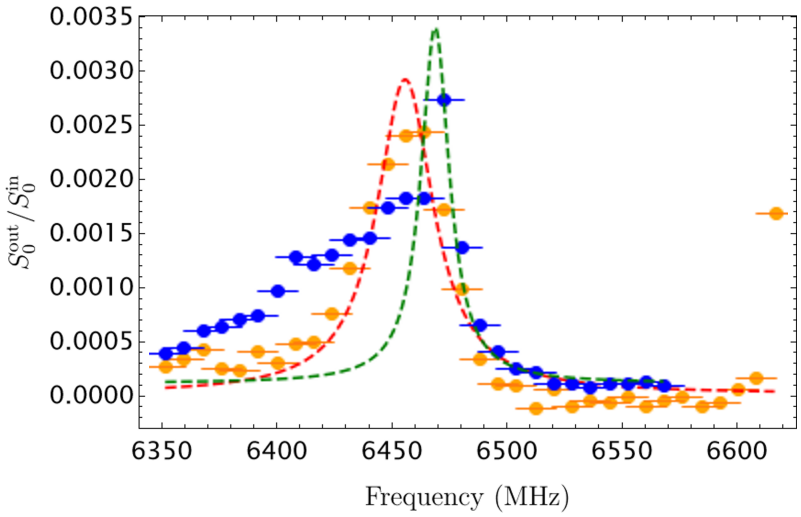

Figure 10: Frequency vs transmission of the probe laser. In blue and in orange the experimental data of the scan before and after the long run of the MSA. in red and green are the fit data for each set. The peak before is centered in 6428MHz and the peak after is centered in 6456MHz

As we can see in figure 10, we scanned the cavity before the first run and after the last one. We can see that the resonance frequency indeed varies through the day. In this case, the frequency change was about 15MHz. This change occur only in a lapse of two and a half hours. Particularly the day of these measurements the changes in the laboratory were not abrupt as it had not external changes. Then, we can take this change as a lower boundary for the changes that can occur in the laboratory conditions. Also we can see that the shape of the peak changed in shape more than in displacement. This also tells us that the finesse of the cavity suffered a disadjusment during the time of the MSA measurements. This type of changes also influence in the search of the maximum intensity as the MSA can find a local maximum instead of a global one.

In figure 11 we can see the distribution of the total number of photons. With these data we can see the performance of the MSA. The 60% of the data is located between 0.001 and 0.0013 of the total transmission. Which means the algorithm is locking close to the maximum transmission 60% of the times. However, the rest 40% is not locking in the right place either because of the Algorithm or because of external factors.

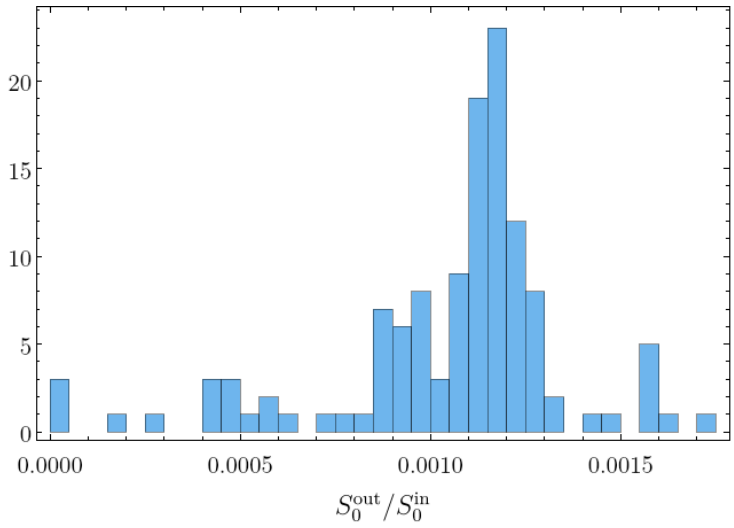

Figure 11: Distribution of the transmission after each experimental run. The transmission was measured with only one side of the differential photodetector.

We can also see that the maximum transmission we can get with the algorithm is also directly correlated with the PD_{Lock} signal as shown in figure 12. We can observe that there are some values that fall far away from this correlation. Let us remind that the signal comming from de PD_{Lock} is the reference on the MSA to do the lock. If the MSA receives the maximum signal from the PD_{Lock}, it will lock the frequency at that value where it should be also the maximum transmission in the DPD. However we can see that there are several cases where this does not occur. Although the MSA is recieving and locking at the maximum value, the transmission measurement will not be necessarily correspondent. For this reason, and for the values outside the 60% range, we believe that there are some other external factors that are influencing the locking between the MSA and the transmission measurement.

The first one is that it is possible that the error signal at the time of the transmission measurements is not stable or has a sudden variation that will change the cavity lock. Another reason could be that the electronic noise in the PD is varying during the sampling time, triggering the MSA to lock at an incorrect value. Although we try to optimize the parameters to take on account the PD noise for the frequency step change($\Delta\nu$), the threshold for the noise (ϵ) and the threshold for the triggering (γ), there are still some values that should not trigger the MSA but they do. However, there is still work on progress. We are planning on recording the error signal for the cavity locking while the MSA and transmission data are being measured. This way we will know when the cavity is unstable and post-select those measurements. Other way to establish the error origin for the MSA is to implement a lock-and-hold locking for the cavity. That way the cavity variations should be diminished and the measurements should be more stable.

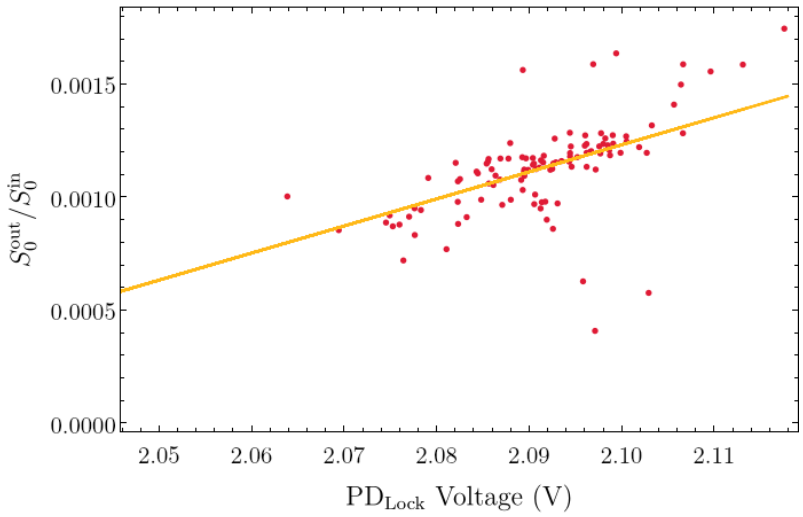

Figure 12: PD_{lock} voltage vs transmission. The transmission was measured with one side of the differential photo detector. The voltage from the PD_{lock} is the reading of the photodetector by the Arduino. The signal coming from the PD_{lock} is the reference that indicates the MSA the transmitted intensity at the locking point

4 Conclusions and further work

In this thesis, the primary objective was to stabilize probe frequency with respect to the cavity length using the transmitted intensity. For this purpose we have designed a Maximum Search Algorithm using a micro-controller Arduino UNO. We tested the performance of the MSA in two set-ups. From the first test set-up we can conclude that in a continuous locking, with an external addition of pink noise, the MSA reduced the mean noise level by 25.37dBm.

On the other hand, the second set-up was implemented into the main experiment. As the main experiment contains the optical cavity, we needed to characterize it. We aligned the cavity so that the TEM_{00} mode for both lasers to be at maximum resonance in the cavity. For the alignment shown in figure 6 we found a finesse of 17.93 for the probe laser and 11.80 for the master laser. The FSR gave us a length of $L = 0.6942 \pm 0.0057$ with a beam waist of $w_o = 21.51\mu$m.

In the main experiment we decided to do a lock-and-hold type of locking system. For this purpose we implemented a rotating mirror with a servomotor and triggered by the Arduino. This way we did not lose any power after the cavity so the MSA has enough intensity to distinguish the peak.

For the implementation set-up we also find a mean noise reduction in the spectrum of 15.23dBm when it was on the continuous configuration. Nevertheless, we needed to measure the stability of the system in a lapse. For this measurements we run a long sequence of three hours with a locking loop every minute. The measurements we got tell us that, although the MSA was trying to lock at the maximum intensity, there were sometimes that the transmission of the cavity was not at the highest. We conclude that there could be several factors that could be influencing the locking. As we are working with the lock-and-hold for the probe laser and a continuous locking for the cavity, it could be that at the time of the sampling, the error signal for the PDH was not stable enough. We also conclude that there are some limitations regarding the algorithm. As we are using a PD, it can be introducing some noise that is limiting our precise maximum intensity. Also, the noise of the PD is limiting the $\Delta\nu$ that we can optimize for the MSA.

For a further work we are going to evaluate if the locking parameters for the cavity could be improved. Besides, we want to implement a lock-and-hold system for the cavity so we can take the measurements with all the locking systems on hold. That way we expect to reduce the variance due to sudden changes.

Although the final objective of this work was to measure magnetic observables in a cold atomic ensemble, we still need to solve the problem of locking stability so the shot noise measurements can be consistent. After the locking problem is solved, we can then take the data for the cavity noise to see if the technical noise has been reduced. If that would not be the case, we would need to reanalyze the system to see which other possibilities can be limiting our detection.

Bibliography

[AEJ+16] C. S. Arridge, J. P. Eastwood, C. M. Jackman, G.-K. Poh, J. A. Slavin, M. F. Thomsen, N. André, X. Jia, A. Kidder, L. Lamy, A. Radioti, D. B. Reisenfeld, N. Sergis, M. Volwerk, A. P. Walsh, P. Zarka, A. J. Coates, and M. K. Dougherty. Cassini in situ observations of long-duration magnetic reconnection in saturn's magnetotail. *Nature Physics*, 12:268–271, 3 2016.

[BCN+14] Justin G. Bohnet, Kevin C. Cox, Matthew A. Norcia, John M. Weiner, Z. Chen, and James K. Thompson. Reduced spin measurement back-action for a phase sensitivity ten times beyond the standard quantum limit. *Nature Photonics*, 8:731–736, 9 2014.

[BK96] Vladimir B. Braginsky and Farid Ya. Khalili. Quantum nondemolition measurements: the route from toys to tools. *Reviews of Modern Physics*, 68:1–11, 1 1996.

[BK13] D Budker and Derek F Jackson Kimball. *Optical Magnetometry*, volume 37. 2013.

[BKR+00] D. Budker, D. F. Kimball, S. M. Rochester, V. V. Yashchuk, and M. Zolotorev. Sensitive magnetometry based on nonlinear magneto-optical rotation. *Physical Review A*, 62:043403, 9 2000.

[Bla01] Eric D. Black. An introduction to pound–drever–hall laser frequency stabilization. *American Journal of Physics*, 69:79–87, 1 2001.

[BMS+17] Elena Boto, Sofie S. Meyer, Vishal Shah, Orang Alem, Svenja Knappe, Peter Kruger, T. Mark Fromhold, Mark Lim, Paul M. Glover, Peter G. Morris, Richard Bowtell, Gareth R. Barnes, and Matthew J. Brookes. A new generation of magnetoencephalography: Room temperature measurements using optically-pumped magnetometers. *NeuroImage*, 149:404–414, 4 2017.

[CBW+14] Zilong Chen, Justin G. Bohnet, Joshua M. Weiner, Kevin C. Cox, and James K. Thompson. Cavity-aided nondemolition measurements for atom counting and spin squeezing. *Physical Review A*, 89:043837, 4 2014.

[CCSM16] Ferran Martin Ciurana, Giorgio Colangelo, Robert J. Sewell, and Morgan W. Mitchell. Real-time shot-noise-limited differential photodetection for atomic quantum control. *Optics Letters*, 41:2946, 7 2016.

[DB09] Matt. R. Dietrich and B. B. Blinov. Use of a microcontroller for fast feedback control of a fiber laser. *arXiv preprint arXiv:0905.2484*, 5 2009.

[dE+15] Y. Natali Martinez de Escobar, Silvana Palacios Álvarez, Simon Coop, Thomas Vanderbruggen, Krzysztof T. Kaczmarek, and Morgan W. Mitchell. Absolute frequency references at 1529 and 1560nm using modulation transfer spectroscopy. *Optics Letters*, 40:4731–4734, 10 2015.

[DHK+83] R. W. P. Drever, J. L. Hall, F. V. Kowalski, J. Hough, G. M. Ford, A. J. Munley, and H. Ward. Laser phase and frequency stabilization using an optical resonator. *Applied Physics B Photophysics and Laser Chemistry*, 31:97–105, 6 1983.

[GLP98] Philippe Grangier, Juan A. Levenson, and Jean-Philippe Poizat. Quantum non-demolition measurements in optics. *Nature*, 396(6711):537–542, dec 1998.

[Gue90] Robert D Guenther. Modern optics john wiley & sons. *Inc., New York*, 1990.

[HJR+14] Kaibin Huang, Hanna Le Jeannic, J. Ruaudel, O. Morin, and Julien Laurat. Microcontroller-based locking in optics experiments. *Review of Scientific Instruments*, 85:123112, 12 2014.

[KNDM10] M. Koschorreck, M. Napolitano, B. Dubost, and M. W. Mitchell. Sub-projection-noise sensitivity in broadband atomic magnetometry. *Physical Review Letters*, 104(9):1–4, 2010.

[Maz23] Chiara Mazzinghi. *Cavity-Enhanced Non-Destructive Measurements of Atomic Magnetism*. 2023.

[MOG+21] Chiara Mazzinghi, Daniel Benedicto Orenes, Pau Gomez, Vito G. Lucivero, Enes Aybar, Stuti Gugnani, and Morgan W. Mitchell. Cavity-enhanced polarization rotation measurements for low-disturbance probing of atoms. *Optics Express*, 29:40854, 12 2021.

[MP20] Morgan W. Mitchell and Silvana Palacios Alvarez. Colloquium: Quantum limits to the energy resolution of magnetic field sensors. *Reviews of Modern Physics*, 92(2):21001, 2020.

[Pla07] S Plaszczynski. Generating long streams of $1/f^{\alpha}$ noise. *Fluctuation and Noise Letters*, 07:R1–R13, 3 2007.

[PSO+18] Luca Pezzè, Augusto Smerzi, Markus K. Oberthaler, Roman Schmied, and Philipp Treutlein. Quantum metrology with nonclassical states of atomic ensembles. *Reviews of Modern Physics*, 90(3):035005, sep 2018.

[SCP+11] B. M. Sparkes, Helen M. Chrzanowski, D. P. Parrain, Ben C. Buchler, Ping K. Lam, and Thomas Symul. A scalable, self-analyzing digital locking system for use on quantum optics experiments. *Review of Scientific Instruments*, 82:075113, 7 2011.

[SD14] Martin Suter and Peter Dietiker. Calculation of the finesse of an ideal fabry–perot resonator. *Applied Optics*, 53:7004–7010, 10 2014.

[Ál17] Silvana Palacios Álvarez. *Single domain spinor Bose-Einstein condensate*. ICFO-UPC, 2017.

A Arduino algorithm

```
1
2
3  ////////////////////////////////////////////
4  //               LIBRARIES                //
5
6  #include <analogShield.h>
7  #include <Servo.h>
8
9
10 ////////////////////////////////////////////
11 //      VARIABLES FOR LOCKING SYSTEM      //
12
13 const int freqChannel = 0; // Analog shield channel in which the frequency modulator is c
14 const int photoDetectorOneChannel = 0; // Analog shield channel in which the PD1 is conne
15 int c = 25; // number of data taken for each intensity value
16 float staticIntensity = 65000.0;
17 float startingVoltage;
18 static float staticVoltage = 32593.5;
19 static float epsilon = 8;
20 static float epsilonY = 2;
21 boolean lock = false;
22 float newVoltage;
23 static float minusDeltaStep = 0.2;
24 static float plusDeltaStep = 0.2;
25 float steps = 0;
26 float y1;
27 float y2;
28 int startPin = 7;
29 int start;
30 boolean toPython;
31
32 ////////////////////////////////////////////
33 //          VARIABLES FOR MIRROR          //
34
35 Servo servo;
36 const byte numChars = 32;
37 char receivedChars[numChars];
38
39 ////////////////////////////////////////////
40 //            NEEDED FUNCTIONS            //
41
42
43 // Analog to Digital value function converter
44 float  analogToDigitalConverter(float x){
45   //float conv = 32593.5 + 6605.61*x;
46   float conv = 6605.61*x;
47   return conv;
```

```
}
float  analogToDigitalConverterv2(float x){
  float conv = 32593.5 + 6605.61*x;
  //float conv = 6605.61*x;
  return conv;
}

// Digital to analog value function converter
float  digitalToAnalogConverter(float x){
  float  conv = (x-31987.57)*5 / 31987.57;
  return conv;
}

// Read PD
float readData(){
  float pd1 = 0.0;
  for(int n = 0; n < (int)c+1 ; n++){ //Sample taking
      pd1 = pd1 + analog.read(0);
  }
  return pd1/(c+1);
}
// Search functions
float rightSearch(){
  while(y2 > y1){
    //Serial.println("y2 wins");
    y1 = y2;
    steps = steps + plusDeltaStep;
    newVoltage = startingVoltage + analogToDigitalConverter(steps);
    if(newVoltage > 0 && newVoltage < 65621.55 ){
      analog.write(freqChannel,newVoltage);
    }else{
      newVoltage = staticVoltage;
      steps = 0;
    }
    y2 = readData();
  }
  staticIntensity = y1;
  return newVoltage;
}

float leftSearch(){
  while(y2 < y1){
    //Serial.println("y1 wins");
    y2 = y1;
    steps = steps - minusDeltaStep;
    newVoltage = startingVoltage + analogToDigitalConverter(steps);
    if(newVoltage > 0 && newVoltage < 65621.55 ){
      analog.write(freqChannel,newVoltage);
    }else{
```

```
97        newVoltage = staticVoltage;
98        steps = 0;
99      }
100     y1 = readData();
101   }
102   staticIntensity = y2;
103   return newVoltage;
104 }
105
106 float sweepSearch(){
107   startingVoltage = analogToDigitalConverterv2(-4.9);
108   analog.write(freqChannel,startingVoltage);
109   steps = 0;
110   while(abs(y2 - y1) < epsilonY){
111     y1 = readData();
112     steps = steps + 2*plusDeltaStep;
113     newVoltage = startingVoltage + analogToDigitalConverter(steps);
114     if(newVoltage > 0 && newVoltage < 65621.55 ){
115       analog.write(freqChannel,newVoltage);
116     }else{
117       newVoltage = startingVoltage;
118       steps = 0;
119     }
120     y2 = readData();
121   }
122   return newVoltage;
123 }
124
125 boolean checkMax(float checkVoltage){
126   analog.write(freqChannel,checkVoltage);
127   float check = readData();
128   analog.write(freqChannel,checkVoltage - analogToDigitalConverter(2*minusDeltaStep));
129   float checkLeft = readData();
130   analog.write(freqChannel,checkVoltage + analogToDigitalConverter(2*plusDeltaStep));
131   float checkRight = readData();
132   if((abs(checkLeft - check) < epsilon) && (abs(checkRight - check) < epsilon) ){
133     return true;
134   }else{
135     return false;
136   }
137 }
138
139 ////////////////////////////////////////////
140 //              MAIN PROGRAM              //
141
142
143 void setup() {
144   Serial.begin(9600);
145   analog.begin(); // Start shield
```

```
146   servo.attach(9,544,2300); //Start servo
147   pinMode(startPin,INPUT);
148   servo.write(100); //Go servo to 100 degrees
149   startingVoltage = staticVoltage; //Start point in intensity for max search
150   analog.write(freqChannel,startingVoltage); //Start AOM at centered point
151   newVoltage = startingVoltage; //Start point in voltage of max search
152   lock = false; //Unlock the algorithm
153   toPython = false; //Dont send anything to python yet
154 }
155
156 void loop() {
157   start = digitalRead(startPin);
158   if(start == 1){
159     servo.write(240);
160     if(toPython == false){
161       toPython  = true;
162     }
163     delay(500);
164     y1 = readData();
165     if((abs(staticIntensity - y1) > epsilon ) || y1 < 33700 ){
166       lock = false;
167       startingVoltage = newVoltage;
168       steps = 0;
169     }
170     while(lock == false){
171       steps = steps + plusDeltaStep;
172       newVoltage = startingVoltage + analogToDigitalConverter(steps);
173       if(newVoltage > 0 && newVoltage < 65621.55 ){
174         analog.write(freqChannel,newVoltage);
175       }
176       y2 = readData();
177       //Serial.println("y1");
178       //Serial.println("y2");
179       //Serial.println(y1);
180       //Serial.println(y2);
181       if((y2 - y1) > epsilonY){
182         newVoltage = rightSearch();
183         lock = true;
184       }else if((y1 - y2) > epsilonY){
185         newVoltage = leftSearch();
186         lock = true;
187       }else{
188         startingVoltage = sweepSearch();
189         //Serial.println("sweep");
190         lock = false;
191       }
192     }
193     if(lock == true){
194       //lock = checkMax(newVoltage);
```

```
195         if(y2 < 46050){
196           lock == false;
197         }
198 
199         //Serial.println("final y2");
200         //Serial.println((y2));
201         //Serial.println((newVoltage));
202       }
203     }else if(start == 0){
204       servo.write(100);
205       if(toPython == true){
206         toPython = false;
207         analog.write(freqChannel,newVoltage);
208         Serial.println(newVoltage);
209         Serial.println(y2);
210       }
211     }
212 }
```